Published in final edited form as:
Arch Biochem Biophys. 2014 March 1; 545: 154–161. doi:10.1016/j.abb.2014.01.021.

Dynamic Fluid Flow Stimulation on Cortical Bone and Alterations of the Gene Expressions of Osteogenic Growth Factors and Transcription Factors in a Rat Functional Disuse Model

Minyi Hu, Ph.D. and **Yi-Xian Qin, Ph.D.**[*]
Dept. of Biomedical Engineering, Stony Brook University, Stony Brook, NY 11794-5281

Abstract

Recently we have developed a dynamic hydraulic stimulation (DHS) as a loading modality to induce anabolic responses in bone. To further study the functional process of DHS regulated bone metabolism, **the objective of this study was to evaluate the effects of DHS on cortical bone and its alterations on gene expressions of osteogenic growth factors and transcription factors as a function of time.** Using a model system of 5-month-old hindlimb suspended (HLS) female Sprague-Dawley rats, DHS was applied to the right tibiae of the stimulated rats with a loading frequency of 2Hz with 30mmHg (p-p) dynamic pressure, 5 days/week, for a total of 28 days. Midshafts of the tibiae were analyzed using μCT and histology. Total RNA was analyzed using RT-PCR on selected osteogenic genes (RUNX2, β-catenin, osteopontin, VEGF, BMP2, IGF-1, and TGF-β) on 3-,7-,14-, and 21-day. Results showed increased Cort.Th and Ct.BV/TV as well as a time-dependable fashion of gradual changes in mRNA levels upon DHS. While DHS-driven fold changes of the mRNA levels remained low before Day-7, its fold changes started to elevate by Day-14 and then dropped by Day-21. This study further delineates the underlying molecular mechanism of DHS-derived mechanical signals, and its time dependent optimization.

Keywords

bone microarchitecture; cell signaling; bone mechanotransduction; transcription factors; osteoporosis; osteogenic growth factors

Introduction

Physical regulation plays a critical role in skeletal growth and function. This function involves the perception of extracellular signals and their transformation into intracellular molecular activities. Increasing the surrounding mechanical signals directly activates signaling pathways that promote chondro- and osteoblastic differentiation and proliferation, which further regulate bone metabolism (1–3). In contrast, unchanged or reduced bone

[*]Corresponding Author: Yi-Xian Qin, Ph.D., Dept. of Biomedical Engineering, Stony Brook University, Bioengineering Bldg., Rm 215, Stony Brook, NY 11794-5281, Phone: 631-632-1481, Fax: 631-632-8577, Yi-Xian.Qin@stonybrook.edu.

Disclosure:
All authors state that they have no conflicts of interest.

formation and increased matrix resorption by osteoclasts can result from reduced or absence of mechanical stimuli (1,4,5). Therefore, based on mechanical loading as a powerful anabolic stimulus for bone, interventional modalities delivering mechanical signals to the skeleton can provide an alternate non-pharmacological approach to treat disuse osteoporosis.

Dynamic hydraulic stimulation (DHS) is a recently developed, non-invasive loading modality as a potential countermeasure for osteopenia/osteoporosis. DHS is achieved through an inflatable cuff placed around the hindlimb of an experimental rat. The inflation and deflation of the cuff provide external dynamic pressure compressions with established pressure magnitudes and loading frequencies. Demonstrating in a 4-week functional disuse hindlimb suspension (HLS) rat model, 2Hz DHS with 30mmHg static pressure + 30mmHg (p-p) dynamic pressure for 20 min/day, 5 days/week was able to mitigate tibial trabecular bone loss under such disuse condition (6). Direct intramedullary pressure (ImP) and strain measurements using surgical approach further suggested the possible mechanism of DHS-driven trabecular bone adaptation. Local ImP, with minimal strain, can be generated by oscillatory DHS as a function of stimulation frequency, where the induced dynamic ImP may later enhance bone fluid flow (BFF) (7). To further study the functional process of DHS-derived mechanical signals in bone metabolism, the objective of the present study was to evaluate the effects of DHS on disuse cortical bone and the alterations of the gene expressions of osteogenic growth factors and transcription factors. These effects may underlie the response to the mechanical stimuli derived from DHS, i.e. eliciting downstream molecular response.

Secretion of growth factors following mechanical stimulation aid to trigger bone regeneration. Some of the most potent growth factors include the transforming growth factor-β (TGF-β), the insulin-like growth factors (IGFs), the bone morphogenetic protein-2 (BMP-2) (8,9), and vascular endothelial growth factor (VEGF) (8,10). Functions of these growth factors include enhancement of osteoprogenitor cells' and osteoblasts' proliferation during bone regeneration (9,11), involvement in marrow stromal cells regulated osteoblast proliferation and osteoblastogenesis induction (9,12), facilitation of the differentiation of mesenchymal stem cells (MSCs) to osteochondroblastic lineage (11,13), and promotion of osteoblast differentiation and increases of mineralization of regenerated bone (10). Converging with growth factors, intracellular signaling pathways are activated upon mechanical stimulation, which in turn activate transcription factors that promote bone formation (8). Committed osteoprogenitor cells from MSCs further differentiate into osteoblasts, which then express osteoblast phenotypic genes once become mature and functional (14). As a principal transcription factor, RUNX2 regulates osteoblast differentiation (15). Downstream of RUNX2, β-catenin is a transcription factor that contributes to the control of osteoblastogenesis (16). Other transcription factors, such as osteopontin, modulate both osteoblastic and osteoclastic functions in response to cytokines and mechanical signals (17).

Bone formation progresses over time after the initiation of mechanical loading. Within 24 to 48 hours after mechanical loading starts, new osteoblasts lay on the bone surface and contribute to bone formation that is observed after 96 hours of loading. Bone formation follows a time-dependent manner, in which it increases between 5 and 12 days of loading and returns back to baseline levels after 6 weeks of loading. These data suggest that the whole cycle of bone formation, including osteoblast recruitment followed by matrix production, lasts for about 5 weeks before declining back to baseline levels (2,18–21). It then becomes an interesting research focus to look into the molecular regulatory mechanism in bone subjected to mechanical loading. However, this mechanism is not fully understood.

Knowing the phenotypic response of trabecular bone to DHS, the present study aimed to confirm the effect of DHS on cortical bone and to elucidate the alterations of the gene expressions of osteogenic growth factors and transcription factors in response to DHS over a time course. It was hypothesized that DHS activates the gene expressions of osteogenic growth factors and transcription factors that are involved in mechanotransduction and bone metabolism, and the sequence of the events is time-dependent. In this study, we evaluated DHS-induced cortical bone thickening over 4 weeks and the expressions of selected osteogenesis related genes over a time course of 3 days, 7 days, 14 days, and 21 days.

Materials and Methods

Animal Study 1

The Institutional Animal Care and Use Committee (IACUC) at Stony Brook University approved all experimental procedures. Thirty-six 5-month-old female Sprague-Dawley virgin rats (Charles River, MA) were used to investigate the effects of DHS on cortical bone adaptation under disuse condition. Animals were housed in 18”x18”x 24” (LxWxH) stainless steel HLS cages with standard rodent chow and water *ad libitum*. The temperature-controlled animal room had a 12:12 hour light:dark cycle. Animals were randomly assigned to three groups: age-matched control (n=14), HLS (n=14), and HLS + DHS (n=8). Functional disuse in the rat hindlimbs was introduced by HLS, with similar procedure as previously described (6). Animal’s tail was cleaned using 70% alcohol and then coated with Tincture of Benzoin. The end of the tail was attached to a piece of surgical tape that forms a loop. Using three strips of elastic adhesive bandage to secure the surgical tape, the loop was linked to a tail harness apparatus and a swivel hook which allowed suspension from the top of the cage. With an approximately 30° head-down tilt, the animal’s hindlimbs were about 2 cm above ground while their forelimbs were fully allowed for movements. Animals’ body weights and overall health were carefully monitored throughout the entire study.

Animal Study 2

Ninety-six 5-month-old female Sprague-Dawley virgin rats (Charles River, MA) were used to investigate the alterations of the gene expressions of osteogenic growth factors and transcription factors in response to DHS. The housing condition of the animals and the HLS procedure were the same as in Animal Study 1. The groups of the animals were: 1) age-matched – day 3 (n = 8), 2) HLS – day 3 (n = 8), 3) HLS + DHS – day 3 (n = 8), 4) age-matched – day 7 (n = 8), 5) HLS – day 7 (n = 8), 6) HLS + DHS – day 7 (n = 8); 7) age-matched – day 14 (n = 8), 8) HLS – day 14 (n = 8), 9) HLS + DHS – day 14 (n = 8), 10) age-matched – day 21 (n = 8), 11) HLS – day 21 (n = 8), 12) HLS + DHS – day 21 (n = 8).

DHS Loading Protocols

For both Animal Study 1 and Animal Study 2, daily DHS was applied to the stimulated animals in conjunction with HLS. With the similar setup as in a previous study (6), DHS was delivered to the right tibia by placing a costume-made inflatable cuff around the right hindlimb over the tibia. Dynamic frequencies and magnitudes were controlled through an actuator-driven syringe connected to a programmable 100 MHz waveform/signal generator (Model 395, Wavetek). DHS was given with a stimulation frequency of 2 Hz and a magnitude of 30 mmHg static pressure + 30 mmHg (p-p) dynamic pressures. For Animal Study 1, the daily stimulation of “10 min on – 5 min off – 10 min on” was applied to each stimulated animal while under anesthesia (isoflurane inhalation) 5 days/week, for 4 weeks. For Animal Study 2, daily loading regime was set as “10 min on – 5 min off – 10 min on” over a time course of 3 days, 7 days, 14 days, and 21 days. Rats in the 3-day group were stimulated for 2 days, and rats in the other groups were stimulated for 5 days/week. In the end, the rats from both studies were euthanized at the corresponding time points.

μCT Evaluation

For the samples obtained from Animal Study 1, the mid-shaft portions of the tibiae were scanned for cortical bone morphology using a high resolution μCT scanner (μCT-40, SCANCO Medical AG, Bassersdorf, Switzerland) with a spatial resolution of 36μm. All images were evaluated using a Gaussian filter, with sigma of 0.1, support of 1, and threshold of 400. A 2880 μm region of the cortical bone in the mid-shaft region was analyzed for each sample. Values for cortical bone thickness (Cort.Th, mm), periosteal surface (Peri.S, mm^2), and endosteal surface (Endo.S, mm^2) were evaluated for each mid-shaft cortical bone region.

Histology Evaluation

After the μCT scans, the mid-shaft portions of the tibial samples from Animal Study 1 were dehydrated with isopropanol, and then infiltrated and embedded with the mixture of methyl methacrylate, benzoyl peroxide, and n-butyl phthalate. The samples were sectioned to 8 μm slices cross-sectional using a microtome (Leica 2165, Wetzlar, Germany). Osteomeasure software (OsteoMetrics Inc., Decatur, GA) was used to perform histology evaluation of the mid-shaft cortical bone by tracing the bone images. Histological bone volume fraction (Ct.BV/TV-Histo, %), cortical bone thickness (Ct.Th-Histo, mm), and cortical marrow area (Ct.Ma.Ar, mm^2) were calculated by the software.

RNA Isolation

The stimulated right tibiae and the age-matched controls were harvested from Animal Study 2 to determine the mRNA levels of the selected genes. The bone marrow within the tibiae was flushed out, and the surrounding soft tissues were dissected out from the bone samples. The bone tissue samples were then incubated immediately in RNAlater RNA Stabilization Reagent (Qiagen) and stored at -80ºC until ready for analysis. The frozen bone samples were ground with a mortar and pestle in an RNeasy Plus lysis buffer while remained frozen. A QIA shredder spin column (Qiagen) was used to remove the tissue debris. Total RNA was collected using a standard procedure with an RNeasy plus mini kit (Qiagen) (22). The total RNA samples were diluted down to 20ng/μl. By using the high capacity cDNA reverse transcription kits (Applied Biosystems), ~200ng of total RNA per sample was reverse transcribed into cDNA.

Quantitative Real-time PCR

After extracting the RNA from the samples of Animal Study 2, Quantitative Real-Time PCR was conducted to examine the expressions of the selected genes (RUNX2, β-catenin, osteopontin, VEGF, BMP2, IGF-1, and TGF-β) along with a housekeeping gene GAPDH as an internal control (Gene Expression Assays, Applied Biosystems). The following quantitative real-time PCR was performed using TaqMan Gene Expression Master Mix Kit (Applied Biosystems) (22). Following the calibration using the GAPDH mRNA levels, the mRNA levels of the HLS and HLS+DHS samples were normalized with the corresponding averaged mRNA levels of the age-matched control samples to derive the relative mRNA fold changes.

Statistical Analysis

Statistical outliers of Animal Study 2 were excluded via Grubbs' test method with Alpha = 0.05 significance level using GraphPad QuickCalcs Outlier Calculator. Specifically, these outliers include HLS – day 3 (n = 2), HLS + DHS – day 3 (n = 1), HLS + DHS – day 7 (n = 2), HLS – day 14 (n = 1), HLS – day 21 (n = 1). Values as mean±SD were used for the statistical analysis of the results. Differences between groups were determined using GraphPad Prism 4.0 Software (GraphPad Software Inc, La Jolla, CA). One-way ANOVA

with Tukey's post-hoc test was performed with normal equal variance to determine the differences among groups. The level of significance is established at $p < 0.05$.

Results

μCT Evaluation

Results of μCT analysis with representative scanned images are shown in Figure 1 for the tibial mid-diaphyseal region. The lack of weight-bearing activity for 4 weeks greatly reduced cortical bone quantity, demonstrated by a 2.21% decrease in Cort.Th compared to the age-matched group. However, animals with DHS loading showed significant improvement in the cortical thickness compared to the disused bone. With DHS loading at 2 Hz, there was an increase in Cort.Th by 5.42% ($p < 0.05$). When compared to age-matched animals, animals received HLS + 2Hz DHS showed a 3.09% increase (Figure 1A). Although not statistically significant, HLS increased Peri.S and decreased Endo.S compared to age-matched controls by 1.14% and 8.9%, respectively. DHS, on the other hand, increased Peri.S and decreased Endo.S compared to HLS by 1.19% and 3.82%, respectively (Figure 1B and C).

Histology Evaluation

The histology data showed great improvements in the histomorphometric Ct.BV/TV and Ct.Th in response to DHS (Figure 2). HLS significantly reduced Ct.BV/TV compared to age-matched controls by 5.33% ($p < 0.01$). However, HLS + 2Hz DHS-treated rats showed significant increases in Ct.BV/TV compared to the HLS group by 7.61% ($p < 0.001$) (Figure 2A). For histomorphometric Ct.Th, the data showed similar trend to Ct.BV/TV, although it was not statistical significant. HLS reduced the Ct.Th by 9.92% compared to age-matched controls, while DHS was able to mitigate this reduction by 9.42% compared to HLS (Figure 2B). In addition, HLS induced a 7.29% increase of Ct.Ma.Ar compared to age-matched control, while DHS treatment reduced 22.90% compared to HLS (Figure 2C).

mRNA Levels in the Tibiae – Day 3

After the first three days, HLS greatly reduced the mRNA levels of all the selected genes compared to age-matched controls (Figure 3). For instance, the fold change of the HLS group was lowered by 51%, 89%, 87%, 61%, 70%, 47%, and 86% compared to age-matched controls, respective to RUNX2, β-catenin, osteopontin, VEGF, BMP2, IGF-1, and TGF-β. At this stage, the effect of DHS was not obvious, where the mRNA levels in the DHS-treated group were similar to the HLS group for most of the selected genes, except for RUNX2. Interestingly, RUNX2 mRNA level of the DHS-treated group was 59% lower compared to the HLS group.

mRNA Levels in the Tibiae – Day 7

By day 7, the overall reduction of the mRNA levels in the HLS group compared to age-matched controls was lower than the day-3 data (Figure 4). At this stage, HLS reduced the mRNA of the selected genes by 28%, 24%, 44%, 21%, 31%, 26%, and 21% compared to age-matched controls respective to RUNX2, β-catenin, osteopontin, VEGF, BMP2, IGF-1, and TGF-β. The mRNA levels of the DHS-treated group of all the selected genes remained low. For instance, the fold change of the DHS-treated group was 0.06 (RUNX2), 0.04 (β-catenin), 0.54 (osteopontin), 0.07 (VEGF), 0.05 (BMP2), 0.05 (IGF-1), and 0.05 (TGF-β).

mRNA Levels in the Tibiae – Day 14

By day 14, the selected genes in the DHS-treated group were greatly upregulated. For instance, the fold change of the DHS-treated group was 3.0 (RUNX2), 4.5 (β-catenin), 3.5

(osteopontin), 3.5 (VEGF), 3.7 (BMP2), 4.6 (IGF-1), and 3.2 (TGF-β) Comparing to the HLS group, the DHS-driven fold change increased by 64%, 94% 102%, 187%, 79%, 102%, and 44% respective to RUNX2, β-catenin, osteopontin, VEGF, BMP2, IGF-1, and TGF-β (Figure 5).

mRNA Levels in the Tibiae – Day 21

By day 21, the elevated mRNA levels of the DHS-treated group were slightly less pronounced compared to the day-14 data. Specifically, the DHS-driven fold change was 1.2 (RUNX2), 2.4 (β-catenin), 1.8 (osteopontin), 1.9 (VEGF), 2.5 (BMP2), 2.2 (IGF-1), and 2.4 (TGF-β). By comparing to the HLS group, the DHS-driven fold change increased by 110%, 80% 128%, 60%, -8%, 92%, and 14%, respective to RUNX2, β-catenin, osteopontin, VEGF, BMP2, IGF-1, and TGF-β (Figure 6).

Discussion

The present study evaluated the phenotypic changes on cortical bone tissue and described the osteogenic gene expression analyses of load-driven responses to a novel form of mechanical loading - DHS, in which its mitigation effect on disuse trabecular bone loss had been demonstrated in a previous study (6). Specifically, daily DHS treatment with low magnitude and frequency on hindlimb suspended rats significantly mitigated disuse related reductions in cortical bone volume and thickness of the loaded bone. Longitudinal real-time PCR analysis of the selected osteogenesis related genes showed an interesting time-dependent behavior of DHS loading on encountering the gene suppression under disuse condition. The time-dependent changes of the expressions of the osteogenesis related genes by DHS outlined their potential contributions to the phenotypic changes in the bone tissue, which provided us a deeper understanding on the underlying mechanotransductive mechanism. The external DHS loading may directly couple with oscillatory marrow fluid pressure and further lead to influences in BFF, regulating skeletal mechanotransductive mechanisms that ultimately lead to bone formation.

DHS provided direct circular compressions with low pressure magnitude on the surrounding soft tissues which eliminate matrix deformation. This had been demonstrated in one of our recent publications, which showed that DHS over a range of loading frequencies induced local ImP within the loaded bone without generating bone strain (7). DHS provided low-magnitude loads on the tibial diaphysis while its compressions may potentially alter the pressure within the marrow cavity, influencing BFF related bone adaptation. In the present study, it was shown that the compressions of DHS directly stimulated the periosteal surface and increased its surface area compared to the HLS group. The microCT Endo.S and histological Ct.Ma.Ar both showed a strong trend of the positive effect of DHS loading on the endosteal surface of the cortical mid-shaft, which contributed to the thickening of the cortical bone. Based on the muscle pump theory, DHS may compress the veins within the skeletal muscle and increase the vasculature pressure gradient that promotes capillary blood flow in bone (23–25). Increase of capillary filtration may further increase ImP and induce BFF that ultimately promote bone regeneration (26).

Bone formation by osteoblasts is one of the crucial steps of bone remodeling, which is an essential function for continuous bone renewal to maintain the structural integrity and metabolic capacity of the skeleton throughout one’s lifetime (8). Osteoblasts are originated from MSCs and form the bone multicellular unit with other bone-forming cells (e.g. osteocytes and bone-lining cells), bone-resorbing cells (e.g. osteoclasts), and their progenitor cells and associated cells (e.g. endothelial cells) (27–29). The growth and differentiation of MSCs towards osteoblastogenesis play a critical role in bone regeneration, and this process is determined by a complex array of growth factors and intracellular signaling (8). Since

MSCs are mostly located in bone marrow, ImP induction by DHS delivers mechanical signals that may ultimately stimulate MSC growth and differentiation towards osteoblastogenesis, which ultimately benefits the bone formation on the endosteal surface. Further, the “cambium layer” of the periosteum is full of adult mesenchymal skeletal progenitor cells that provide bone forming and regenerative capacity (43,44). Mechanical signals derived from the direct DHS compressions may also stimulate these cells and increase bone formation on the periosteal surface. Interesting, beneficial effects of DHS in bone formation was observed on both endosteal and periosteal surfaces in the present study.

Augmented external biomechanical stimulation, such as DHS in the present study, may trigger the secretion of growth factors that act as local regulators for osteogenesis. Potent growth factors, including IGF, TGF-β, BMP and VEGF, strongly modulate the osteoblastic activities as well as other bone growth regulators (8). IGF-1 has been shown to trigger proliferation of osteoblasts, which contributes to a gradual bone mass gain *in vivo* (9,30). Committed bone cell replication and matrix synthesis of osteoblast can be induced by TGF-β (31–33). The replication of early bone precursors and osteoblast differentiation commitment can be influenced by BMP-2 (9,34,35). VEGF has been suggested as a promoter for osteoblast differentiation and bone mineralization (10,36). Moreover, activation of intracellular signal transduction pathways and growth factors converge to activate transcription factors. For example, RUNX2 regulates osteoblast differentiation, whereas β-catenin that acts downstream of RUNX2 contributes to the control of osteoblastogenesis (8). Osteopontin is necessary for mechanical stress-dependent signals take effects to bone marrow cells in bone (37). Altogether, these genes play critical roles in the fate of osteoblastogenesis, which is crucial for bone formation. In the current study, amplification of expression of these genes was observed upon DHS over 14 days, strongly indicating the anabolic effect of DHS in bone.

Studies have shown that significantly altered gene expressions of 140 osteogenesis related genes, including RUNX2 in 2T3 preosteoblasts, was observed under weightlessness condition. Specifically, only 3 days of unloading decreased the mRNA levels of ALP, RUNX2, and PTHR1 by 5, 2, and 5 fold, respectively (38,39). Similar observations were seen in our present study. By day 3 of HLS, unloaded tibial bones showed greatly reduced mRNA levels of the selected osteogenesis-related genes. This observed reduction continued over 21 days.

On the other hand, studies of mechanical loading have demonstrated the effect of BFF stimulation on growth factor and transcription factor expression levels. For instance, *in vitro* cyclic and static stretching of osteoblasts (MC3T3-E1) was shown to increase IGF-mediated signaling, leading to differentiation of late osteoblasts and early osteocytes (9,30). Mechanical strains of 2000 με on human osteoblast-like cells (SaOS-2) induced bone-forming indices, whereas strains of 200,000 – 300,000 με led to reductions (31–33). Inductions of BMP-mediated up-regulation of RUNX2 and smad1 phosphorylation were observed in human SaOS in response to compression force. BMP mRNA level was elevated by *in vitro* sinusoidal cyclic stretch on human spinal ligament cells (9,34,35). In cultured osteoblasts, load-driven up-regulation of ALP and RUNX2 has been reported in cultured osteoblasts (39–41). Our present study showed mechanical loading-dependent up-regulation of the mRNA levels of the selected genes in an *in vivo* setting. By 14 days, pronounced increases in the mRNA levels of the selected genes were shown in the DHS-treated group compared to the HLS group. This increase of gene expressions continued but started to diminish by 21 days. Our group previously presented a longitudinal study of bone marrow MSC quantification under DHS in a rat HLS model, where the MSC number was greatly increased in response to DHS by day 14 and diminished by day 21. MSCs may have completed proliferation and begin to differentiate towards osteoblastogenesis at this stage. In

the meantime, the induced mRNA levels of the selected genes that we observed in the present study couples the process of transforming MSC proliferation and differentiation into osteoblasts, which commit to the subsequent bone formation. Strong mitigation effect of DHS on disuse trabecular bone loss has been demonstrated in our previous published work. Altogether, the *in vivo* study on the phenotypic change in the bone tissue as well as the longitudinal studies on bone marrow MSC quantification and mRNA levels of osteogenesis related genes compile these events as a sequential pathway of how DHS exerts its mechanical signals to bone cells. How bone cells respond to such stimuli contributes to the phenotypic change in bone.

Interestingly, DHS did not counteract the reduction of the osteogenic gene expressions at the earlier time points (e.g. 3 days and 7 days), while these mRNA levels of the HLS groups rebound and approached to the levels of the age-matched levels starting from Day 7 (Figure 7). The HLS and HLS+DHS groups present different patterns and time frames of osteoblastogenic gene expressions in response to HLS and HLS+DHS, respectively. By incorporating the longitudinal bone marrow MSC quantification data during the first 7 days, bone marrow MSCs of the HLS+DHS group seemed to actively proliferate and the total MSC number increased compared to HLS group (42). A strong time-dependent manner of bone marrow MSC induction was observed in response to DHS, which peaked on Day 14. Based on the sequential events of MSC proliferation and differentiation, it is suggesting that since the differentiation process had not begun yet, expressions of the osteogenesis related genes were still inactive.

In summary, this study indicated that the mRNA levels of the selected osteogenesis related genes were positively influenced by the mechanical signals derived from DHS generated BFF, which provides important understanding of the downstream molecular mechanism of DHS on bone adaptation. The mRNA expression has demonstrated the loading time dependent function, in which the optimized response of mRNA peaked at two weeks following the initial bone fluid flow loading. This implies that DHS is not only a novel, non-invasive intervention for regulating skeletal adaptation, but also serves as a unique signal to trigger the molecular mechanotransduction process in response to fluid flow stimuli in bone. Future directions include analysis of DHS mechanotransduction on other cell types, such as osteocytes for their mechano-sensing property. Further investigations, such as temporal MSC differentiation analysis, are also needed to fully understand the interrelationships between bone tissue response, MSC proliferation and differentiation, and the underlying molecular response of bone cells and progenitor cells. Furthermore, while the current PCR data were mainly derived from the cortical bone region, it would be in great relevant to also derive PCR data from the surrounding soft tissues, e.g. muscles, to study the bone-muscle interrelationship related to in vivo observations.

Acknowledgments

This research is kindly supported by the National Institute of Health (R01 AR52379 and AR61821), the US Army Medical Research and Materiel Command, and the National Space Biomedical Research Institute through NASA Cooperative Agreement NCC 9-58. The authors are grateful to Michelle Lien and Alyssa Tuthill for their excellent technical supports.

References

1. Papachristou DJ, Papachroni KK, Basdra EK, Papavassiliou AG. Signaling networks and transcription factors regulating mechanotransduction in bone. Bioessays. 2009; 31(7):794–804. [PubMed: 19444851]
2. Schriefer JL, Warden SJ, Saxon LK, Robling AG, Turner CH. Cellular accommodation and the response of bone to mechanical loading. J Biomech. 2005; 38(9):1838–45. [PubMed: 16023471]

3. Ng AF, Yang YO, Wong RW, Hagg EU, Rabie AB. Factors regulating condylar cartilage growth under repeated load application. Front Biosci. 2006; 11:949–54. [PubMed: 16146785]
4. Huiskes R, Ruimerman R, van Lenthe GH, Janssen JD. Effects of mechanical forces on maintenance and adaptation of form in trabecular bone. Nature. 2000; 405(6787):704–6. [PubMed: 10864330]
5. Kreja L, Liedert A, Hasni S, Claes L, Ignatius A. Mechanical regulation of osteoclastic genes in human osteoblasts. Biochem Biophys Res Commun. 2008; 368(3):582–7. [PubMed: 18243138]
6. Hu M, Cheng J, Qin YX. Dynamic hydraulic flow stimulation on mitigation of trabecular bone loss in a rat functional disuse model. Bone. 2012; 51(4):819–25. [PubMed: 22820398]
7. Hu M, Serra-Hsu F, Bethel N, Lin L, Ferreri S, Cheng J, Qin YX. Dynamic hydraulic fluid stimulation regulated intramedullary pressure. Bone. 2013; 57(1):137–141. [PubMed: 23895997]
8. Papachroni KK, Karatzas DN, Papavassiliou KA, Basdra EK, Papavassiliou AG. Mechanotransduction in osteoblast regulation and bone disease. Trends Mol Med. 2009; 15 (5): 208–16. [PubMed: 19362057]
9. Bikle DD. Integrins, insulin like growth factors, and the skeletal response to load. Osteoporos Int. 2008; 19(9):1237–46. [PubMed: 18373051]
10. Zelzer E, Olsen BR. Multiple roles of vascular endothelial growth factor (VEGF) in skeletal development, growth, and repair. Curr Top Dev Biol. 2005; 65:169–87. [PubMed: 15642383]
11. Lieberman JR, Daluiski A, Einhorn TA. The role of growth factors in the repair of bone. Biology and clinical applications. J Bone Joint Surg Am. 2002; 84-A(6):1032–44. [PubMed: 12063342]
12. Zhang RW, Simmons DJ, Crowther RS, Mohan S, Baylink DJ. Contribution of marrow stromal cells to the regulation of osteoblast proliferation in rats: evidence for the involvement of insulin-like growth factors. Bone Miner. 1991; 13(3):201–15. [PubMed: 1863809]
13. Gautschi OP, Frey SP, Zellweger R. Bone morphogenetic proteins in clinical applications. ANZ J Surg. 2007; 77(8):626–31. [PubMed: 17635273]
14. Harada S, Rodan GA. Control of osteoblast function and regulation of bone mass. Nature. 2003; 423(6937):349–55. [PubMed: 12748654]
15. Ziros PG, Basdra EK, Papavassiliou AG. Runx2: of bone and stretch. Int J Biochem Cell Biol. 2008; 40(9):1659–63. [PubMed: 17656144]
16. Marie PJ. Transcription factors controlling osteoblastogenesis. Arch Biochem Biophys. 2008; 473(2):98–105. [PubMed: 18331818]
17. Ishijima M, Tsuji K, Rittling SR, Yamashita T, Kurosawa H, Denhardt DT, Nifuji A, Noda M. Resistance to unloading-induced three-dimensional bone loss in osteopontin-deficient mice. J Bone Miner Res. 2002; 17(4):661–7. [PubMed: 11918223]
18. Turner CH, Owan I, Alvey T, Hulman J, Hock JM. Recruitment and proliferative responses of osteoblasts after mechanical loading in vivo determined using sustained-release bromodeoxyuridine. Bone. 1998; 22(5):463–9. [PubMed: 9600779]
19. Forwood MR, Owan I, Takano Y, Turner CH. Increased bone formation in rat tibiae after a single short period of dynamic loading in vivo. Am J Physiol. 1996; 270(3 Pt 1):E419–23. [PubMed: 8638687]
20. Turner CH, Pavalko FM. Mechanotransduction and functional response of the skeleton to physical stress: the mechanisms and mechanics of bone adaptation. J Orthop Sci. 1998; 3(6):346–55. [PubMed: 9811988]
21. Mantila Roosa SM, Turner CH, Liu Y. Regulatory mechanisms in bone following mechanical loading. Gene Regul Syst Bio. 2012; 6:43–53.
22. Zhang P, Turner CH, Yokota H. Joint loading-driven bone formation and signaling pathways predicted from genome-wide expression profiles. Bone. 2009; 44(5):989–98. [PubMed: 19442616]
23. Winet H. A bone fluid flow hypothesis for muscle pump-driven capillary filtration: II. Proposed role for exercise in erodible scaffold implant incorporation. Eur Cell Mater. 2003; 6:1–10. discussion 10–1. [PubMed: 14562269]
24. Otter MW, Qin YX, Rubin CT, McLeod KJ. Does bone perfusion/reperfusion initiate bone remodeling and the stress fracture syndrome? Med Hypotheses. 1999; 53(5):363–8. [PubMed: 10616033]

25. Laughlin MH. The muscle pump: what question do we want to answer? J Appl Physiol. 2005; 99 (2):774. [PubMed: 16020444]
26. Qin YX, Lam H, Ferreri S, Rubin C. Dynamic skeletal muscle stimulation and its potential in bone adaptation. J Musculoskelet Neuronal Interact. 2010; 10(1):12–24. [PubMed: 20190376]
27. Abdallah BM, Kassem M. Human mesenchymal stem cells: from basic biology to clinical applications. Gene Ther. 2008; 15(2):109–16. [PubMed: 17989700]
28. Heino TJ, Hentunen TA. Differentiation of osteoblasts and osteocytes from mesenchymal stem cells. Curr Stem Cell Res Ther. 2008; 3(2):131–45. [PubMed: 18473879]
29. Frost HM. Bone's mechanostat: a 2003 update. Anat Rec A Discov Mol Cell Evol Biol. 2003; 275(2):1081–101. [PubMed: 14613308]
30. Tang LL, Xian CY, Wang YL. The MGF expression of osteoblasts in response to mechanical overload. Arch Oral Biol. 2006; 51(12):1080–5. [PubMed: 16934742]
31. Ahdjoudj S, Lasmoles F, Holy X, Zerath E, Marie PJ. Transforming growth factor beta2 inhibits adipocyte differentiation induced by skeletal unloading in rat bone marrow stroma. J Bone Miner Res. 2002; 17(4):668–77. [PubMed: 11918224]
32. Ito Y, Miyazono K. RUNX transcription factors as key targets of TGF-beta superfamily signaling. Curr Opin Genet Dev. 2003; 13(1):43–7. [PubMed: 12573434]
33. Cillo JE Jr, Gassner R, Koepsel RR, Buckley MJ. Growth factor and cytokine gene expression in mechanically strained human osteoblast-like cells: implications for distraction osteogenesis. Oral Surg Oral Med Oral Pathol Oral Radiol Endod. 2000; 90(2):147–54. [PubMed: 10936833]
34. Zhao G, Monier-Faugere MC, Langub MC, Geng Z, Nakayama T, Pike JW, Chernausek SD, Rosen CJ, Donahue LR, Malluche HH, Fagin JA, Clemens TL. Targeted overexpression of insulin-like growth factor I to osteoblasts of transgenic mice: increased trabecular bone volume without increased osteoblast proliferation. Endocrinology. 2000; 141(7):2674–82. [PubMed: 10875273]
35. Duncan RL. Transduction of mechanical strain in bone. ASGSB Bull. 1995; 8(2):49–62. [PubMed: 11538550]
36. Papadopoulou AK, Papachristou DJ, Chatzopoulos SA, Pirttiniemi P, Papavassiliou AG, Basdra EK. Load application induces changes in the expression levels of Sox-9, FGFR-3 and VEGF in condylar chondrocytes. FEBS Lett. 2007; 581(10):2041–6. [PubMed: 17467696]
37. Ishijima M, Tsuji K, Rittling SR, Yamashita T, Kurosawa H, Denhardt DT, Nifuji A, Ezura Y, Noda M. Osteopontin is required for mechanical stress-dependent signals to bone marrow cells. J Endocrinol. 2007; 193(2):235–43. [PubMed: 17470514]
38. Pardo SJ, Patel MJ, Sykes MC, Platt MO, Boyd NL, Sorescu GP, Xu M, van Loon JJ, Wang MD, Jo H. Simulated microgravity using the Random Positioning Machine inhibits differentiation and alters gene expression profiles of 2T3 preosteoblasts. Am J Physiol Cell Physiol. 2005; 288(6):C1211–21. [PubMed: 15689415]
39. Zhang P, Hamamura K, Yokota H. A brief review of bone adaptation to unloading. Genomics Proteomics Bioinformatics. 2008; 6(1):4–7. [PubMed: 18558381]
40. Patel MJ, Liu W, Sykes MC, Ward NE, Risin SA, Risin D, Jo H. Identification of mechanosensitive genes in osteoblasts by comparative microarray studies using the rotating wall vessel and the random positioning machine. J Cell Biochem. 2007; 101(3):587–99. [PubMed: 17243119]
41. Kanno T, Takahashi T, Tsujisawa T, Ariyoshi W, Nishihara T. Mechanical stress-mediated Runx2 activation is dependent on Ras/ERK1/2 MAPK signaling in osteoblasts. J Cell Biochem. 2007; 101(5):1266–77. [PubMed: 17265428]
42. Hu M, Yeh R, Lien M, Teeratananon M, Agarwal K, Qin YX. Dynamic Fluid Flow Mechanical Stimulation Modulates Bone Marrow Mesenchymal Stem Cells. Bone Research. 2013; (1):98–104.
43. Allen MR, Hock JM, Burr DB. Periosteum: biology, regulation, and response to osteoporosis therapies. Bone Nov. 2004; 35(5):1003–12.
44. Lin Z, Fateh A, Salem DM, Intini G. Periosteum: Biology and Applications in Craniofacial Bone Regeneration. J Dent Res. 2013 Oct 2.

Highlights

- Dynamic hydraulic stimulation (DHS) increased Cort.Th, Ct.BV/TV, and mRNA levels in a time dependent fashion.
- DHS-driven fold changes of the mRNA levels remained low before Day-7.
- Fold changes of mRNA were elevated by Day-14 and then dropped by Day-21.
- This study investigated the possible mechanism of DHS-derived mechanical signals.

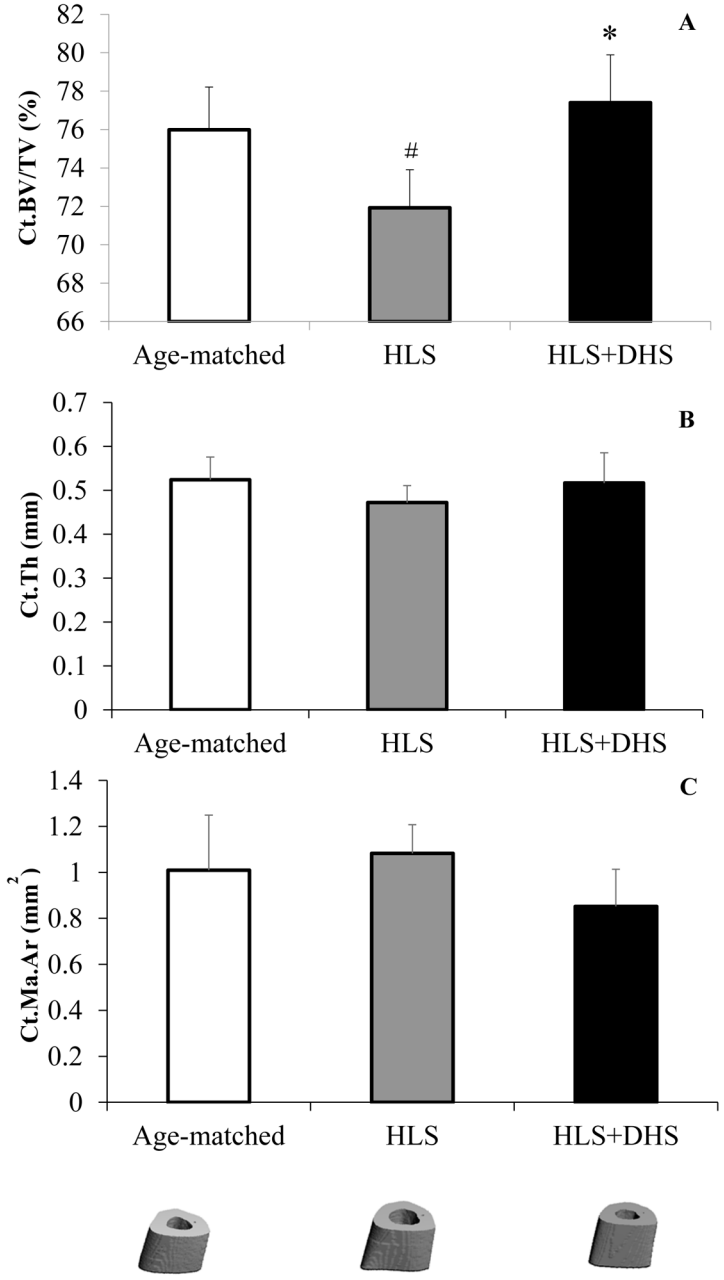

Figure 1.

Graphs show mean±SD values for A) cortical bone thickness (Cort.Th, mm), B) periosteal surface (Peri.S, mm^2), C) endosteal surface (Endo.S, mm^2), and representative 3D μCT images of mid-diaphyseal region of the tibiae. DHS at 2 Hz produced a significant change in Cort.Th, compared to values obtained in 4-week HLS. *$p < 0.05$ vs. HLS.

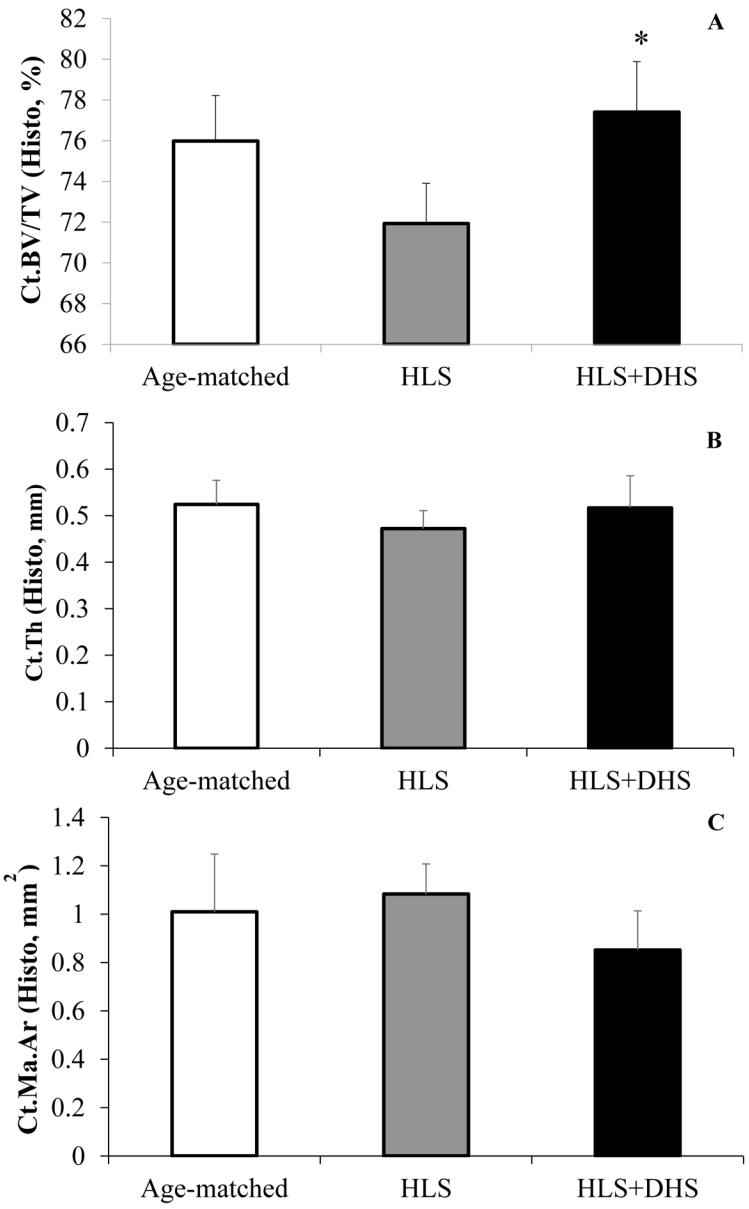

Figure 2.

Histology analysis on tibial mid-diaphysis. Values are mean±SD. A) HLS significantly reduced Ct.BV/TV compared to age-matched controls, while HLS + 2Hz DHS-treated rats showed significant increases in Ct.BV/TV compared to the HLS group. B) HLS reduced the Ct.Th compared to age-matched controls, while DHS loading at 2 Hz was able to mitigate this reduction. C) HLS increased Ct.Ma.Ar compared to age-matched controls, while 2Hz DHS loading mitigated disuse related marrow space expansion. $^{\#}p < 0.01$ vs. age-matched; $^{*}p < 0.001$ vs. HLS.

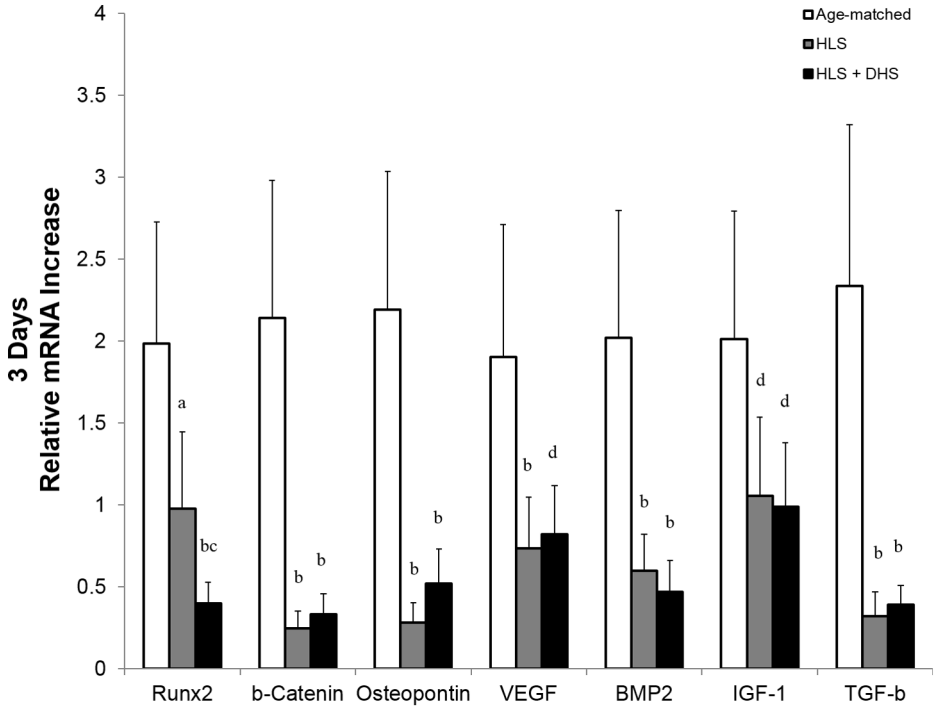

Figure 3.

Graphs show mean±SE of mRNA levels in the tibiae – day 3. Hindlimb suspension (HLS) greatly reduced the mRNA levels of all the selected genes compared to age-matched controls. The effect of DHS was not obvious, where the mRNA levels in the DHS-treated group were similar to the HLS group for most of the selected genes, except for RUNX2. [a]$p < 0.01$ vs. age-matched; [b]$p < 0.001$ vs. age-matched; [c]$p < 0.01$ vs. HLS; [d]$p < 0.01$ vs. age-matched.

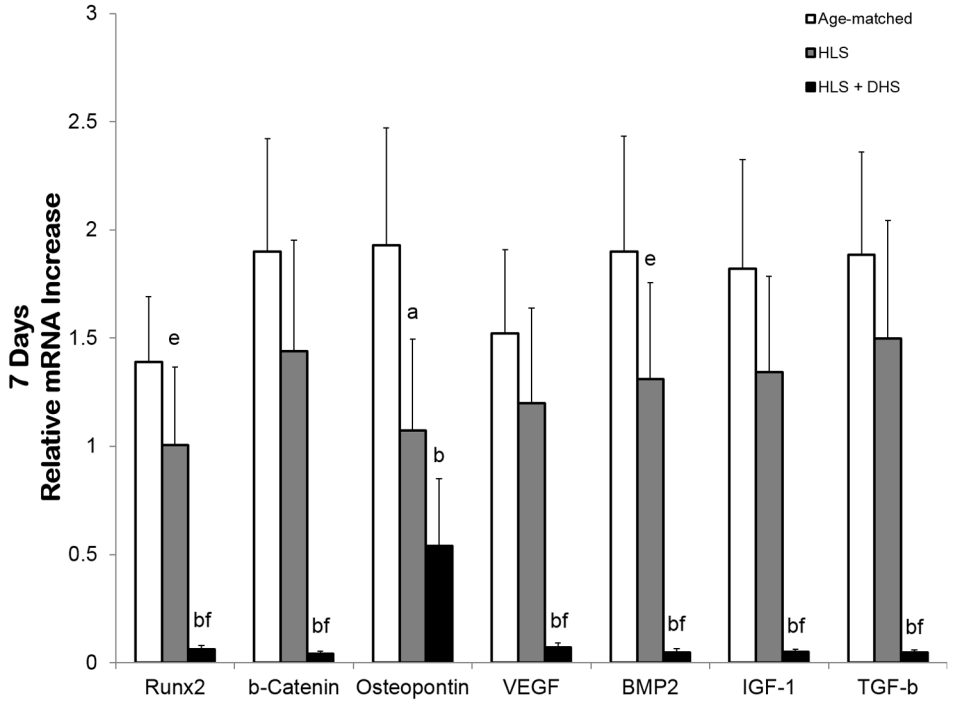

Figure 4.

Graphs show mean±SE of mRNA levels in the tibiae – day 7. The overall reduction of the mRNA levels in the HLS group compared to age-matched controls was lower than the day-3 data. Interestingly, the mRNA levels of DHS-treated group of all the selected genes remained low. [a]$p < 0.01$ vs. age-matched; [b]$p < 0.001$ vs. age-matched; [c]$p < 0.01$ vs. HLS; [d]$p < 0.01$ vs. age-matched; [e]$p < 0.05$ vs. age-matched; [f]$p < 0.001$ vs. HLS.

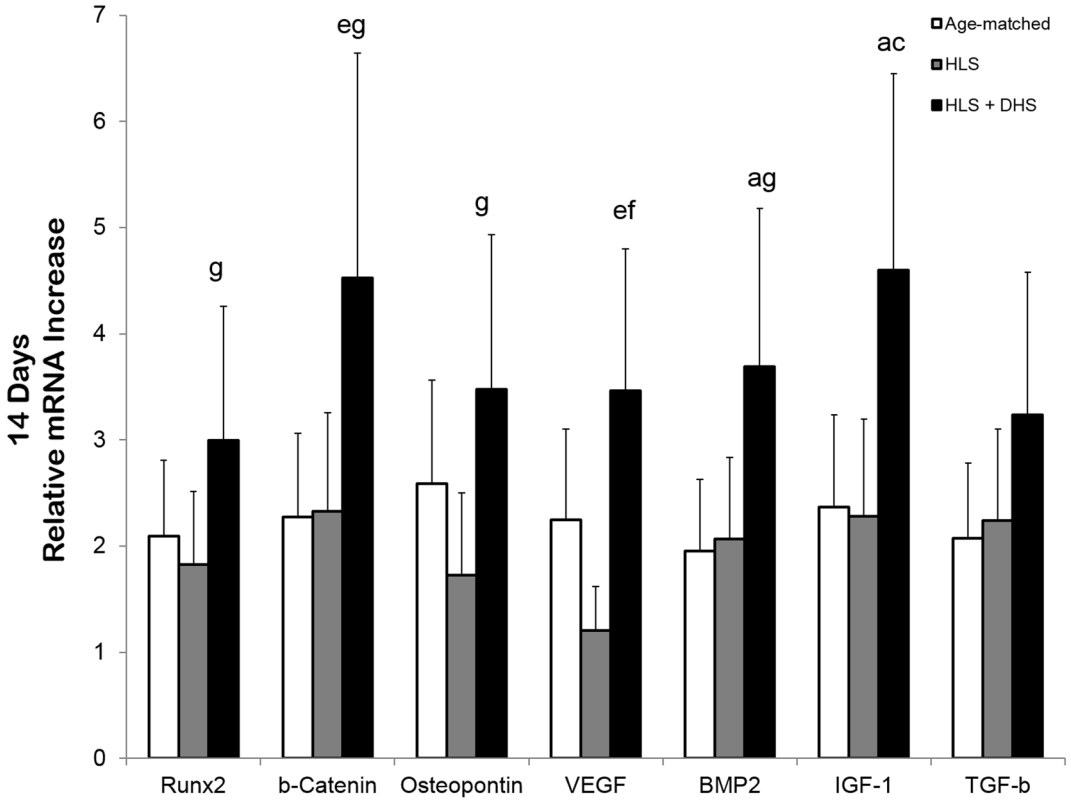

Figure 5.

Graphs show mean±SE of mRNA levels in the tibiae – day 14. The selected genes in the DHS-treated group were greatly upregulated. For instance, the fold change of the DHS-treated group was 3.0 (runx2), 4.5 (β-catenin), 3.5 (osteopontin), 3.5 (VEGF), 3.7 (BMP2), 4.6 (IGF-1), and 3.2 (TGF-β). [a]$p < 0.01$ vs. age-matched; [b]$p < 0.001$ vs. age-matched; [c]$p < 0.01$ vs. HLS; [d]$p < 0.01$ vs. age-matched; [e]$p < 0.05$ vs. age-matched; [f]$p < 0.001$ vs. HLS; [g]$p < 0.05$ vs. HLS.

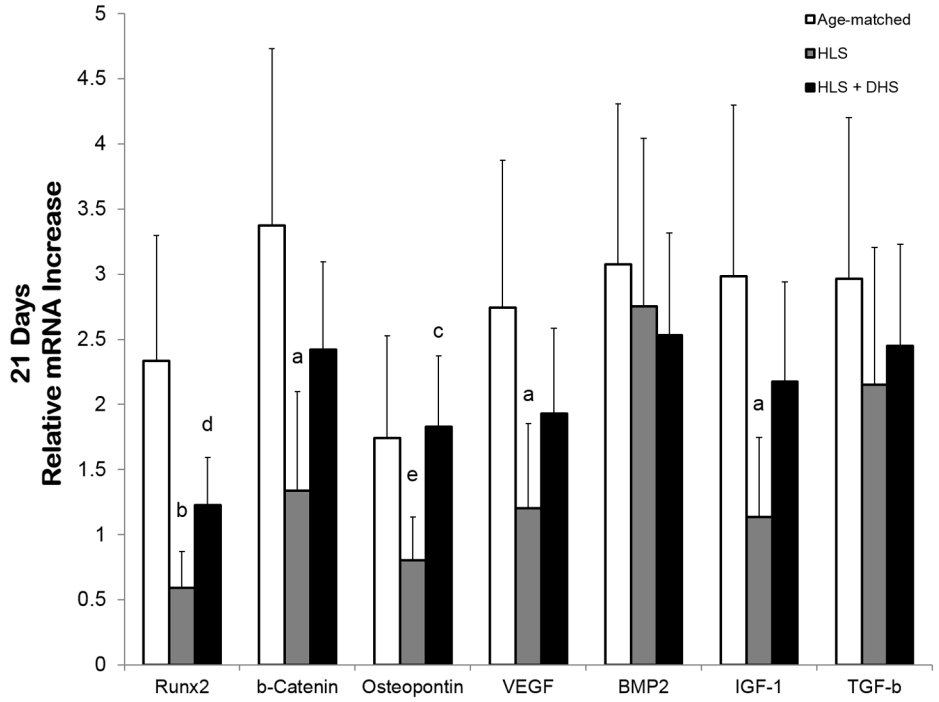

Figure 6.

Graphs show mean±SE of mRNA levels in the tibiae – day 21. The elevated mRNA levels of the DHS-treated group were slightly less pronounced compared to the day-14 data. Specifically, the DHS-driven fold change was 1.2 (RUNX2), 2.4 (β-catenin), 1.8 (osteopontin), 1.9 (VEGF), 2.5 (BMP2), 2.2 (IGF-1), and 2.4 (TGF-β). [a]$p < 0.01$ vs. age-matched; [b]$p < 0.001$ vs. age-matched; [c]$p < 0.01$ vs. HLS; [d]$p < 0.01$ vs. age-matched; [e]$p < 0.05$ vs. age-matched.

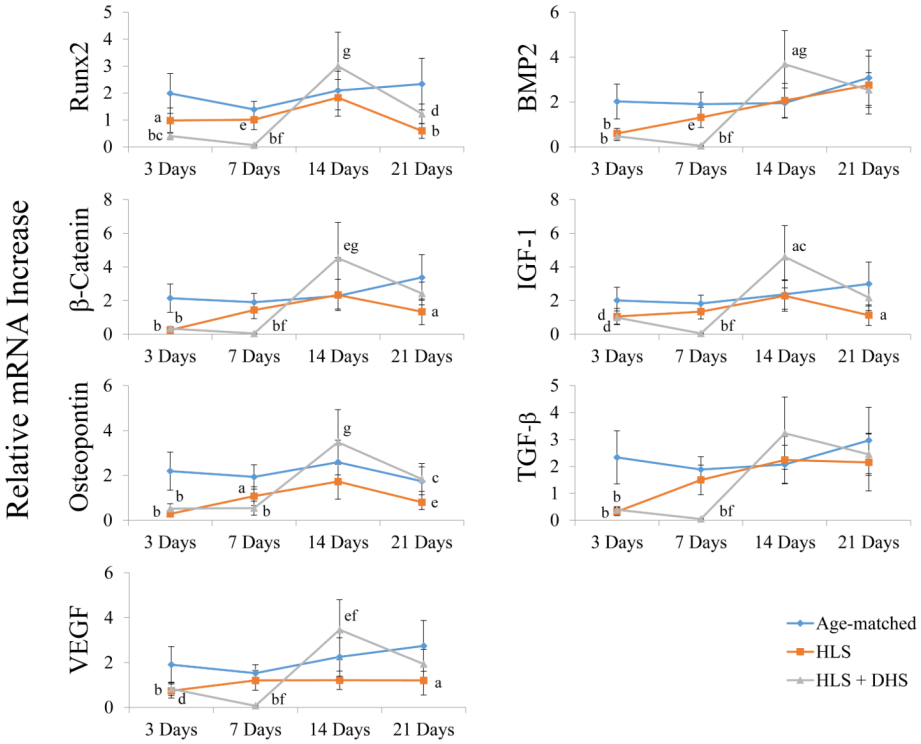

Figure 7.

Summary of mRNA fold changes of the selected osteogenesis related genes over the 21-day time course. Graphs show mean±SE of mRNA levels in the tibiae. In general, the mRNA levels of the selected genes in the HLS groups attempted to catch up to the according age-matched levels. However, the mRNA levels of these genes in the HLS+DHS groups did not elevate until day 14. $^{a}p < 0.01$ vs. age-matched; $^{b}p < 0.001$ vs. age-matched; $^{c}p < 0.01$ vs. HLS; $^{d}p < 0.01$ vs. age-matched; $^{e}p < 0.05$ vs. age-matched; $^{f}p < 0.001$ vs. HLS; $^{g}p < 0.05$ vs. HLS.